Electronic Supplementary Information for

The Role of Adsorbed Hydroxide Reduction in Hydrogen Evolution and Nitrogen Reduction Reactions in Aqueous Solution

Yuan Zhao,*[a,b,†] Min Hu,[b,†] Huirong Li,[b,†] Binhua Chu,[a] Yan Huang,[b] Chuanyi Jia,[c] Zhiwen Zhuo,[d] Yi Luo,[b] Jun Jiang*[,b]

[a] School of Physics and Optoelectronic Engineering, Ludong University, Yantai, Shandong 264025, P. R. China. E-mail: zhaoyuan@ldu.edu.cn

[b] School of Chemistry and Materials Science, University of Science and Technology of China, Hefei, Anhui 230026, P. R. China. E-mail: jiangj1@ustc.edu.cn

[c] Guizhou Provincial Key Laboratory of Computational Nano-Material Science, Institute of Applied Physics, Guizhou Education University, Guiyang, Guizhou 550018, P. R. China.

[d] Department of Physics, Anhui Normal University, Wuhu, Anhui, 241000, P. R. China

† These authors equally contributed to this work.

Computational details

Spin-polarized density functional theory (DFT) method was employed for all calculations using the Perdew−Burke−Ernzerhof (PBE) functional in conjunction with the plane-wave projected augmented wave (PAW) method as implemented in the Vienna ab initio simulation Package program (VASP).[1-4] A plane-wave cutoff energy was set to be 400 eV for all calculations. The first Brillouin zone was sampled using 3 × 3 × 1 k-points for fully relaxed geometry optimization until the maximal residual force was converged to less than 0.02 eV/Å. The vacuum space in the z-direction was set to be 20 Å for preventing the interaction between two neighboring periodic units. The empirical correction in Grimme's scheme was used to describe the van der Waals interaction. It should be noted that the DFT+U method underestimates the intermediate adsorptions (especially for the *OH adsorption energy), which contradicts to the actually strong interactions between transition-metal single-atom and intermediates. Therefore, following the previous works with similar systems of $TMN_{3/4}$ active sites, we used DFT method to study it.[5-7] The calculation of Gibbs reaction free energy of the electrochemical elementary steps was performed by using the computational hydrogen electrode (CHE) model developed by Nørskov and co-workers.[8-10] In this model, we set up reversible hydrogen electrode (RHE) as the reference electrode. Using DFT method, it is extremely difficult to directly calculate the accurate energies of charged species such as proton (H^+), hydroxyl ion (OH^-), and electrons (e^-) involved in electrochemical reactions. Under $P_{H2} = P_0 = 1$ bar, T = 298.15 K, U = 0 V vs. RHE, the electrochemical hydrogen evolution is in the thermodynamic equilibrium ($H^+(aq) + e^- \leftrightarrow 1/2H_2$ (g)). This means that the free energy of proton-electron pairs [$H^+(aq) + e^-$] is equal to the half free energy of H_2 [$(G_{H+(aq)}) + (G_{e-}) = 1/2(G_{H2})$].[8]

The Gibbs free energy change (ΔG) for each element step was calculated as follows,[11-13]

$$\Delta G = \Delta E + \Delta E_{ZPE} - T\Delta S + \Delta G_U + \Delta G_{pH} \quad (1)$$

where ΔE is the energy difference between the products and reactants; ΔE_{ZPE} and ΔS are the changes in the zero-point energy and entropy, respectively. T is the room temperature (T = 298.15 K). The potential effect on the free energy involving an electron in the electrode is taken into account by shifting the energy of the state by ΔG_U = -neU, where U is the electrode applied potential, e is the elementary charge and n is the number of proton–electron pairs transferred. The equilibrium potential U_0 for HER at pH = 7 was determined to be -0.41V vs SHE (standard hydrogen electrode) or 0 V vs RHE at 298.15 K according to Nernst equation ($E = E^0 - 0.059 \times pH$).[13-17] ΔG_{pH} is the free energy correction of pH and it was calculated as $\Delta G_{pH} = k_B T \times pH \times \ln 10$ when the potential is referred to SHE, where k_B is the Boltzmann constant.

The limiting potential (U_L) was calculated via[18]

$$U_L = -\Delta G_{max}/e \quad (2)$$

where ΔG_{max} is the free energy change of potential-determining step (PDS).

References

1. G. Kresse and J. Furthmüller, *Phys. Rev. B*, 1996, **54**, 11169-11186.
2. C. J. M. van der Ham, M. T. M. Koper and D. G. H. Hetterscheid, *Chem. Soc. Rev.*, 2014, **43**, 5183-5191.
3. G. Kresse and D. Joubert, *Phys. Rev. B*, 1999, **59**, 1758-1775.
4. P. E. Blöchl, *Phys. Rev. B*, 1994, **50**, 17953-17979.
5. Y. Wang, Y.-J. Tang and K. Zhou, *J. Am. Chem. Soc.*, 2019, **141**, 14115-14119.
6. M. Xiao, L. Gao, Y. Wang, X. Wang, J. Zhu, Z. Jin, C. Liu, H. Chen, G. Li, J. Ge, Q. He, Z. Wu, Z. Chen and W. Xing, *J. Am. Chem. Soc.*, 2019, **141**, 19800-19806.
7. Y. Li, X. Liu, L. Zheng, J. Shang, X. Wan, R. Hu, X. Guo, S. Hong and J. Shui, *J. Mater. Chem. A*, 2019, **7**, 26147-26153.
8. J. K. Nørskov, J. Rossmeisl, A. Logadottir, L. Lindqvist, J. R. Kitchin, T. Bligaard and H. Jónsson, *J. Phys. Chem. B*, 2004, **108**, 17886-17892.
9. J. Rossmeisl, Z. W. Qu, H. Zhu, G. J. Kroes and J. K. Nørskov, *J. Electroanal. Chem.*, 2007, **607**, 83-89.
10. J. Rossmeisl, A. Logadottir and J. K. Nørskov, *Chem. Phys.*, 2005, **319**, 178-184.
11. A. A. Peterson, F. Abild-Pedersen, F. Studt, J. Rossmeisl and J. K. Nørskov, *Energy Environ. Sci.*, 2010, **3**, 1311-1315.
12. P. Ou, X. Zhou, F. Meng, C. Chen, Y. Chen and J. Song, *Nanoscale*, 2019, **11**, 13600-13611.
13. H. X. Xu, D. J. Cheng, D. P. Cao and X. C. Zeng, *Nat. Catal.*, 2018, **1**, 339-348.
14. J. Gao, H. Tao and B. Liu, *Adv. Mater.*, 2021, **33**, 2003786.
15. F. Lv, J. Feng, K. Wang, Z. Dou, W. Zhang, J. Zhou, C. Yang, M. Luo, Y. Yang, Y. Li, P. Gao and S. Guo, *ACS Central Sci.*, 2018, **4**, 1244-1252.
16. J. Gao, X. Huang, W. Cai, Q. Wang, C. Jia and B. Liu, *ACS Appl. Mater. Interfaces*, 2020, **12**, 25991-26001.
17. Y. Guo, X. Cai, S. Shen, G. Wang and J. Zhang, *J. Catal.*, 2021, **402**, 1-9.
18. J. Chen, H. Cheng, L.-X. Ding and H. Wang, *Mater. Chem. Front.*, 2021, **5**, 5954-5969.
19. Z. Chen, C. Liu, L. Sun and T. Wang, *ACS Catal*, 2022, **12**, 8936-8975.
20. X. Lv, W. Wei, B. Huang, Y. Dai and T. Frauenheim, *Nano Letters*, 2021, **21**, 1871-1878.

The element reaction steps of HER/NRR in aqueous and acidic solution:

The *OH formation and reduction steps in aqueous solution (pH=7)

$* + H_2O \rightarrow *OH + H^+ + e^-$ (ΔG_{*OH})

$*OH \rightarrow * + OH^- - e^-$ ($\Delta G_{*OH\text{-}Red}$)

The HER pathway in acidic solution (pH=0)

$* + H^+ + e^- \rightarrow *H$ (ΔG_{*H})

$*H \rightarrow * + 1/2H_2$ ($1/2\Delta G_{*H2}$)

The HER pathway in aqueous solution (pH=7)

$* + H_2O \rightarrow *H + OH^- - e^-$ (ΔG_{*H})

$*H \rightarrow * + 1/2H_2$ ($1/2\Delta G_{*H2}$)

The NRR-$*N_2$ distal pathway in acidic solution (pH=0)

$* + N_2 \rightarrow *N_2$ (ΔG_{*N2})

$*N_2 + H^+ + e^- \rightarrow *N_2H$ (ΔG_{*N2H})

$*N_2H + H^+ + e^- \rightarrow *NNH_2$ (ΔG_{*NNH2})

$* NNH_2 + H^+ + e^- \rightarrow *N + NH_3$ (g) (ΔG_{*N})

$*N + H^+ + e^- \rightarrow *NH$ (ΔG_{*NH})

$*NH + H^+ + e^- \rightarrow *NH_2$ (ΔG_{*NH2})

$*NH_2 + H^+ + e^- \rightarrow *NH_3$ (ΔG_{*NH3})

$*NH_3 \rightarrow * + NH_3$ (g)

The NRR-$*N_2$ distal pathway in aqueous solution (pH=7)

$* + N_2 \rightarrow *N_2$ (ΔG_{*N2})

$*N_2 + H_2O \rightarrow *N_2H + OH^- - e^-$ (ΔG_{*N2H})

$*N_2H + H_2O \rightarrow *NNH_2 + OH^- - e^-$ (ΔG_{*NNH2})

$*NNH_2 + H_2O \rightarrow *N+NH_3$ (g) $+ OH^- - e^-$ (ΔG_{*N})

$*N + H_2O \rightarrow *NH + OH^- - e^-$ (ΔG_{*NH})

$*NH + H_2O \rightarrow *NH_2 + OH^- - e^-$ (ΔG_{*NH2})

$*NH_2 + H_2O \rightarrow *NH_3 + OH^- - e^-$ (ΔG_{*NH3})

$*NH_3 \rightarrow * + NH_3$ (g)

The NRR-*H pathway in acidic solution (pH=0)

$* + H^+ + e^- \rightarrow *H$ (ΔG_{*H})

$*H + N_2 \rightarrow *N_2H$ (ΔG_{*N2H})

$*N_2H + H^+ + e^- \rightarrow *NHNH$ (ΔG_{*NHNH})

$*NHNH + H^+ + e^- \rightarrow *NHNH_2$ (ΔG_{*NHNH2})

$*NHNH_2 + H^+ + e^- \rightarrow *NH_2NH_2$ ($\Delta G_{*NH2NH2}$)

$*NH_2NH_2 + H^+ + e^- \rightarrow *NH_2 + NH_3$ (g) (ΔG_{*NH2})

$*NH_2 + H^+ + e^- \rightarrow *NH_3$ (ΔG_{*NH3})

$*NH_3 \rightarrow * + NH_3$ (g)

The NRR-*H pathway in aqueous solution (pH=7)

$* + H_2O \rightarrow *H + OH^- - e^-$ (ΔG_{*H})

$*H + N_2 \rightarrow *N_2H$ (ΔG_{*N2H})

$*N_2H + H_2O \rightarrow *NHNH + OH^- - e^-$ (ΔG_{*NHNH})

$*NHNH + H_2O \rightarrow *NHNH_2 + OH^- - e^-$ (ΔG_{*NHNH2})

$*NHNH_2 + H_2O \rightarrow *NH_2NH_2 + OH^- - e^-$ ($\Delta G_{*NH2NH2}$)

$*NH_2NH_2 + H_2O \rightarrow *NH_2 + NH_3$ (g) $+ OH^- - e^-$ (ΔG_{*NH2})

$*NH_2 + H_2O \rightarrow *NH_3 + OH^- - e^-$ (ΔG_{*NH3})

$*NH_3 \rightarrow * + NH_3$ (g)

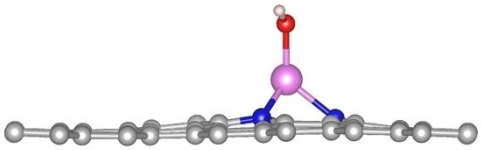

Fig. S1 The optimized atomic structure of *OH for NiN_3.

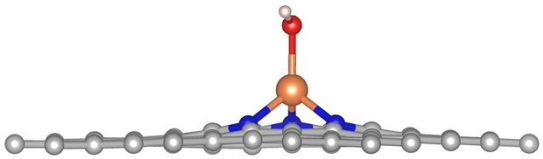

Fig. S2 The optimized atomic structure of *OH for CoN_3.

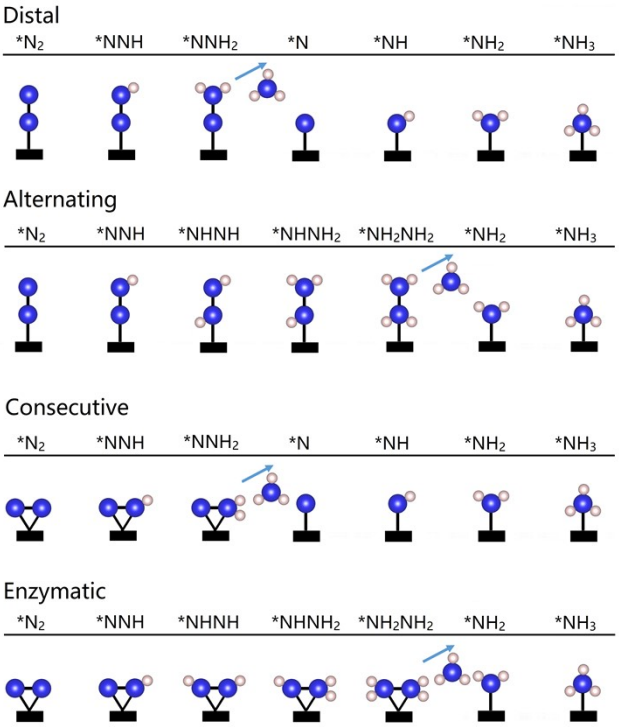

Fig. S3 Schematic illustrations of distal, alternating, consecutive, and enzymatic pathways of NRR.

For associative reaction mechanism, there are usually four different pathways (called as distal, alternating, consecutive, and enzymatic patterns) depending on the binding mode of N_2 and the hydrogenation position of N.[19, 20] Specifically, in distal pathway, the N_2 has an end-on adsorption configuration on the catalyst, and hydrogenation preferably takes place from the remote N atom, where the possible reaction intermediates include *NNH, *NNH_2, *N, *NH, *NH_2, and *NH_3. In alternating pathway, the N_2 also has an end-on adsorption configuration on the catalyst, but hydrogenation starts alternately on two N atoms, where the formations of *NNH, *NHNH, *$NHNH_2$, *NH_2NH_2, *NH_2, and *NH_3 intermediates are possible. In consecutive pathway, the N_2 has a side-on adsorption configuration with both N atoms binding to the catalyst and then undergoes distal hydrogenation steps to produce NH_3. In enzymatic pathway, the N_2 also has a side-on adsorption configuration and then undergoes alternate hydrogenation steps to produce NH_3.

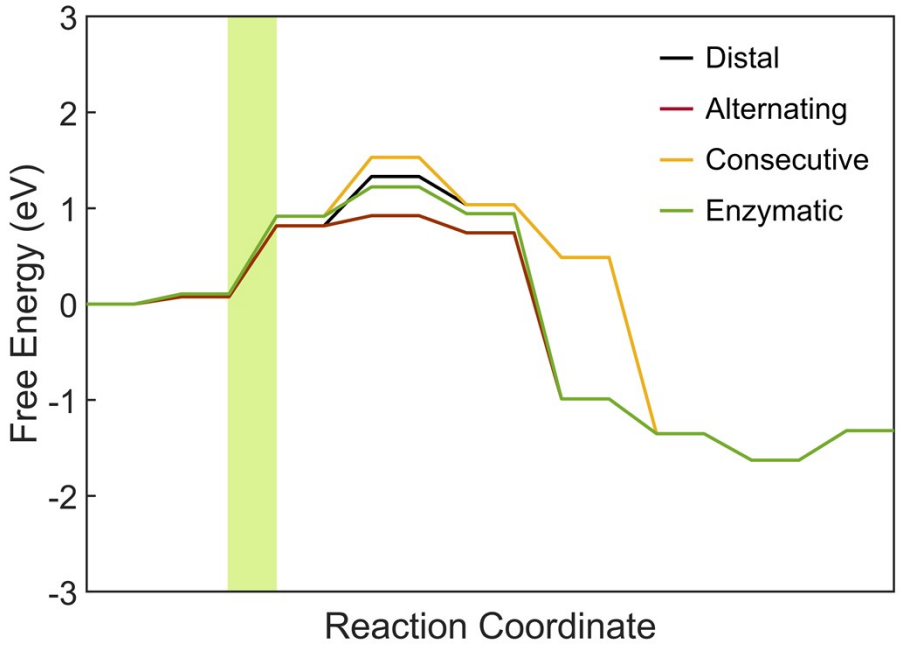

Fig. S4 The calculated free energy profiles of NRR on CoN_3 site with U=0 V through distal, alternating, consecutive and enzymatic pathways. The light green region denotes the potential-determining step (PDS) of four reaction pathways. It should be noted that in the enzymatic pathway, the $*NH_2NH_2$ via the side-on manner is unstable, as it would be optimized to the end-on configuration after full atomic relaxation.

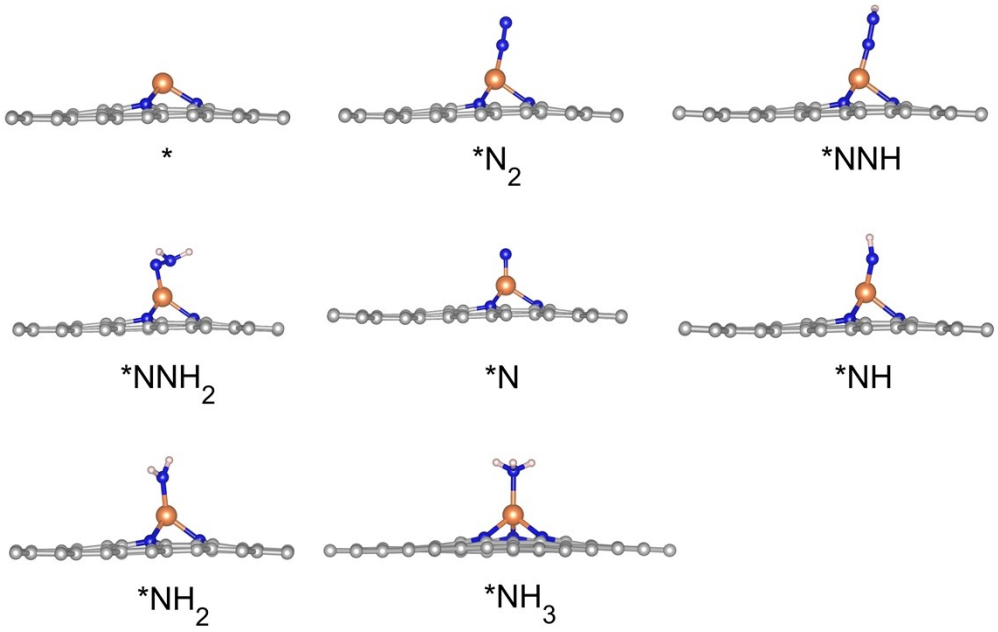

Fig. S5 The optimized atom structures of various intermediates proceeded on CoN_3 along the NRR-*N_2 distal pathway.

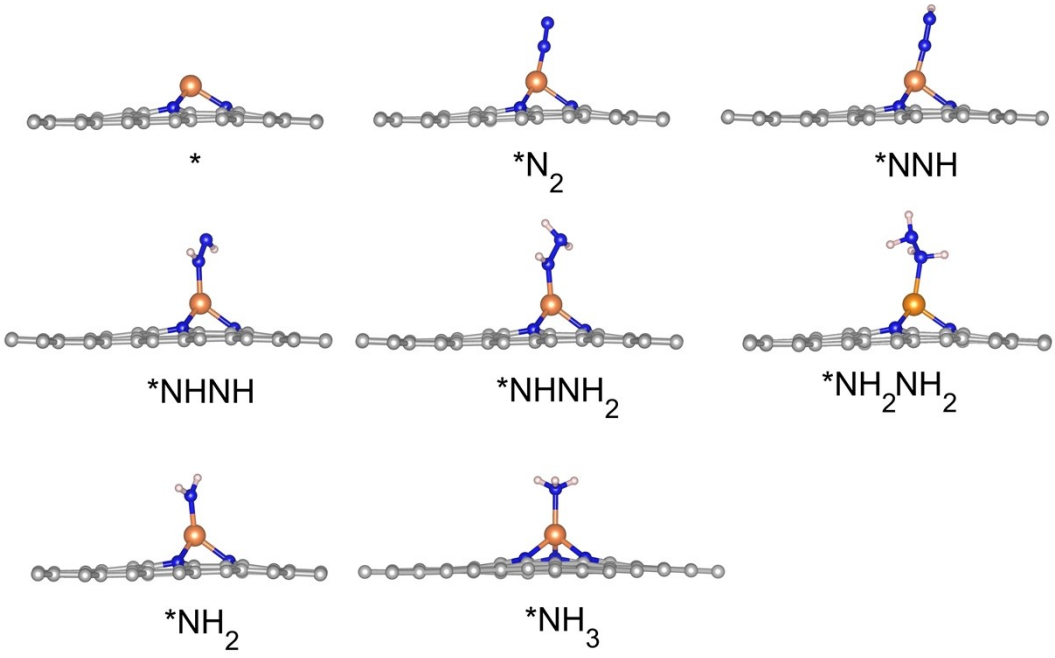

Fig. S6 The optimized atom structures of various intermediates proceeded on CoN_3 along the NRR-*N_2 alternating pathway.

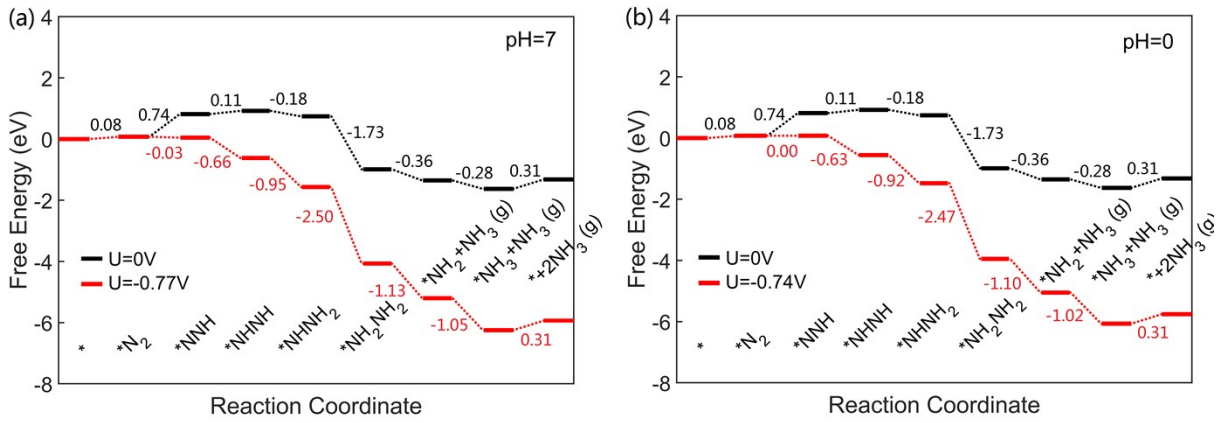

Fig. S7 The free energy profile of NRR-*N_2 alternating pathway on CoN_3 at pH=7 (a) and pH=0 (b). The reference potential is set to be 0 V vs RHE.

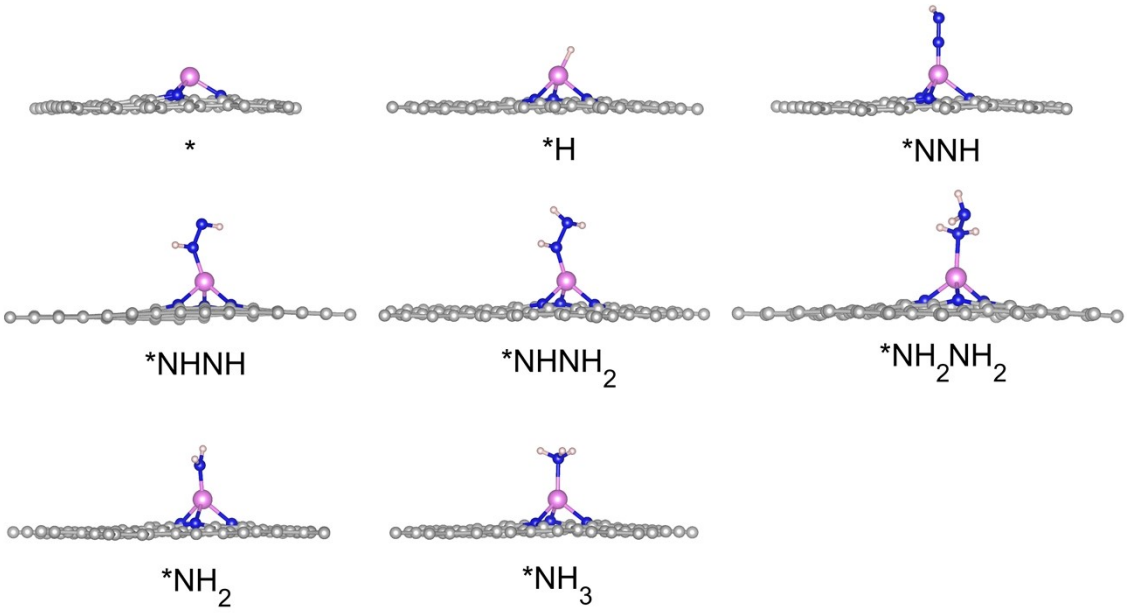

Fig. S8 The optimized atom structures of various intermediates proceeded on NiN_3 along the NRR-*H pathway.